Miniaturized Dehumidifier Integrated with Acetone Breathalyzer

by

Hou-Yu Chen

B. S. in Mechanical Engineering, National Tsing Hua University, 2016

Submitted to the Graduate Faculty of

Swanson School of Engineering in partial fulfillment

of the requirements for the degree of

Master of Science in Mechanical Engineering

University of Pittsburgh

2019

UNIVERSITY OF PITTSBURGH

SWANSON SCHOOL OF ENGINEERING

This thesis was presented

by

Hou-Yu Chen

It was defended on

July 16, 2019

and approved by

Sung Kwon Cho, Ph.D., Professor

Department of Mechanical Engineering and Materials Science

Young Jae Chun, Ph.D., Associate Professor

Department of Industrial Engineering

Sangyoep Lee, Ph.D., Assistant Professor

Department of Mechanical Engineering and Materials Science

Thesis Advisor: Sung Kwon Cho, Ph.D., Professor

Department of Mechanical Engineering and Materials Science

Miniaturized Dehumidifier Integrated with Acetone Breathalyzer

Hou-Yu Chen, M.S.

University of Pittsburgh, 2019

In this article, we are targeting on simulating human breath test on acetone breathalyzer. As increasing amount of literature shows that breath acetone has strong links with human metabolism, health and diets such as nutrition related ketogenic diet. Normal individuals has breath level ranging from 0.5 ppm to 2 ppm. People doing ketogenic diet would increase up to 40 ppm. However, multiple studies point out the acetone sensor response diminished while testing under high humidity level conditions. Therefore, the designed thermoelectric dehumidifier is applied on acetone sensor to remove moisture. The results compared with and without input dehumidified system on acetone concentration tests show that dehumidified process can precise the concentration to 1ppm level at 90 % relative humidity.

For miniaturized dehumidifier to portable size, we introduced SU-8 negative photoresist to create microchannel. Polydimethylsiloxane (PDMS) material contains inert, non-toxic and optical clear properties which dominates the material choices on microfluidic devices. The PDMS microchannel dehumidifier not only reduced humidity levels but minimized dehumidified devices volume.

Table of Contents

List of Figures

Acknowledgements

For over a year to finish my master thesis but without the following people help I couldn't achieve it.

First and foremost, I want to show my thankful to my advisor Dr. Sung Kwon Cho for giving me the opportunity to work in MEMS lab during the past year with my all heart appreciation. All those useful advices inspired me digging for knowledges and try to find my weak side and fix it. Try to learn from every single mistake and correct them. These are priceless. I would also want to thankful for my committee members, Dr. Young Jae Chun and Dr. Sangyeop Lee for the time, support and encouragement for my thesis.

Secondly, I would like to thank my peers in Bio-Engineering, Sean Huang for cooperating with this project. Without your help and advices I would not finish this project. Thank you for all the time you answer my endless questions. And also my lab mate Wenbo as a best ever PHD student. You sacrificed the time during the weekend and help me out the fabrication and taught me some background knowledge I really appreciated. Also Tony, Fangwei, Hongyao and Dr. Hur you guys are amazing for selfless help.

Last but not least, I would want to show my deepest thankful for my family. Thank you for breeding me all the way to study abroad. There is no word to show my appreciation during these years. Also, my sister Jou-Yu you are always my lighthouse to remind me never give up and keep chasing for the bright future.

These will be my best memories in my UPITT study life.

1.0 Introduction

1.1 Acetone Background

Usually Acetone been regarded as a waste product of metabolism. Nowadays instead of doing some invasive tests like blood or urine samples it is more possible to detect human exhaled breath. Human breath contains plenty of volatile organic compounds (VOCs) like acetone and ethanol in exhaled air but most of compounds with very low volume levels which under parts-per-billion volume (ppbv) or even parts-per-trillion volume (pptv). Other than large abundance species like CO_2, water and methane the endogenous acetone production may represent enough information about human beings' metabolic disorders like diabetes mellitus or lung cancer and alcoholism and nutrition related ketogenic diet [1]. They are all highly needed acetone detection in exhaled breath. From the breath acetone spectrum figure X shows that normal healthy individuals breath acetone level can range from 0.5 to 2.0 ppm [2]. Adults with ketogenic diet can range up to 40 ppm. For the diabetes cases the acetone level would elevate up to 1250 ppm.

For measurement of acetone levels there are many instruments on market such as mass spectrometers, gas chromatographs, UV light detection [3], metal oxide sensors and semiconductor-based gas sensor can detect to parts-per-million volume (ppmv) levels. But most of them can only measure 50 ppm level. Yamada [4] using Zeolite to trap and concentrate acetone to reach higher concentration level. However, several technical limitations come out while detecting such as samples storage, standardization and detection threshold [5]. Besides, the humidity level influences acetone sensor precision when in high humidity level [6]. Coyne [7] discusses human inspiratory flow rates and humidity level during hard work or other different

respirator inhalation and exhalation resistances. The results show that human exhalation humidity over 90% RH all the time. Therefore, dehumidifying process and minimizing for acetone breathalyzer is where this research focusing on.

1.2 Humidity Measurement

For measuring the relative humidity (% RH) level the humidity sensor DHT22 is introduced in the project. Relative humidity ratio is the water vapor in the air versus the saturation point of water vapor. The ambient temperature also influences the saturation point. Therefore, the higher the air temperature the more water can be hold at the saturation point. The DHT22 humidity and temperature sensor is able to measure the temperature ranging between -40 to 125°C with less than ±1°C error and relative humidity levels ranging from 0 to 100% with ±2% error [8]. At 100% RH the air reach saturation point where condensation occurs. On the other hand 0% RH means the air is completely dry. By applying our sensor onto Arduino board and 16 by 2 LCD display shows humidity and temperature results as shown in Figure 1. The potentiometer and resistors in Arduino circuit help adjust displaying brightness and contrast.

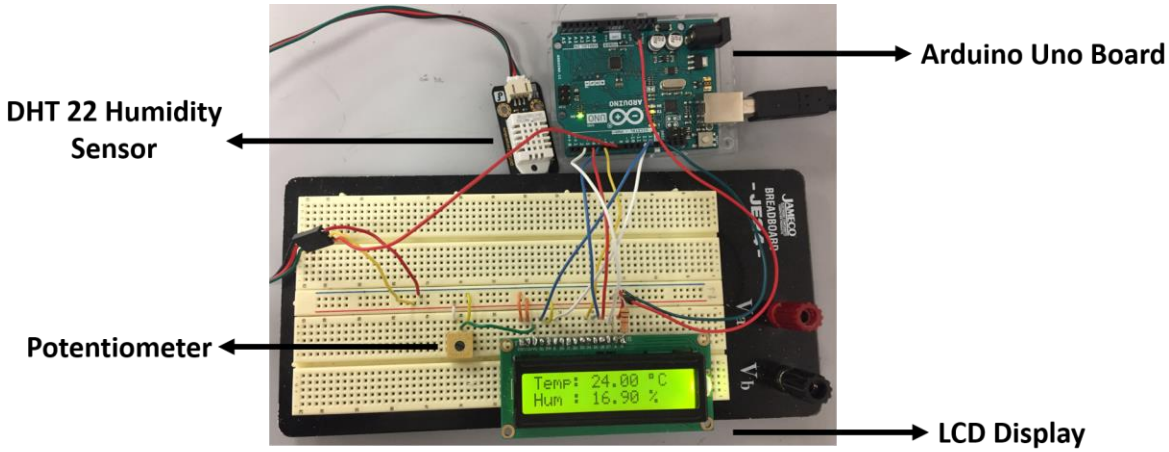

Figure 1 Arduino humidity Sensor

1.3 PDMS Microchannel

In biological microchannels are increasingly used in microvalves and microsensors for analyzing chemical regents or biological cells. Polydimethylsiloxane (PDMS) is the material that contains chemically and biologically inert, non-toxic and optical clear properties [9] which dominates the material choices for microfluidic devices.

1.4 Thermoelectric Cooler

Thermoelectric devices or Peltier devices have been wildly used for refrigerators, infrared sensor and electric cooling devices like CPU [10] . Thermoelectric cooler (TEC) is the device that contains two dissimilar electrical conductors to create temperature gradient on the junction as a heat pump. Generally, the structure of TEC module consists array of semiconductor as shown in

Figure 2. The configuration of pellets is connected in series electrically but parallel in thermally. When the DC current applied to devices the P and N-type Bismuth Telluride in Peltier array would absorb heat from one side and release heat from the other. The substrate surface absorbs heat is called cold side using for refrigerating or condensing humid air. On the other hand, the surface releasing heat is called hot side for removing heat the most commonly used methods are air cooling and liquid cooling [11] . In this project the Peltier module been selected is the model from CUI Inc. CP85438 as shown in Figure 3. While facing thermal fatigue our module has several following benefits. First, thermal resin layer implanted between ceramic surfaces and semiconductors reduces thermal resistance and strengthen system structure. After repeated heating up and cooling down process in resin materials still have superior bonding and good thermal connection. Secondly, better solder material SbSn carries over 200 degree melting point which offers better shear strength compared to traditional solder material and also provides solid connection between thermoelectric pairs. Last characteristic is that larger P/N elements applied on the module would increase cooler surface area and also provide more uniform cooling. All the above improvements enhance TECs performance and reduce the thermal resistance changing rate when in high temperature condition.

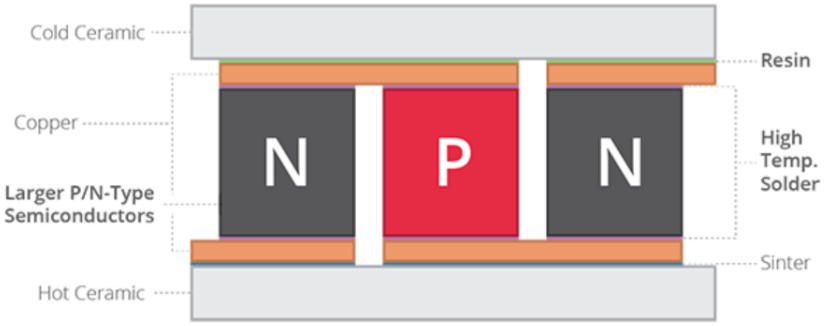

Figure 2 Peltier module structure

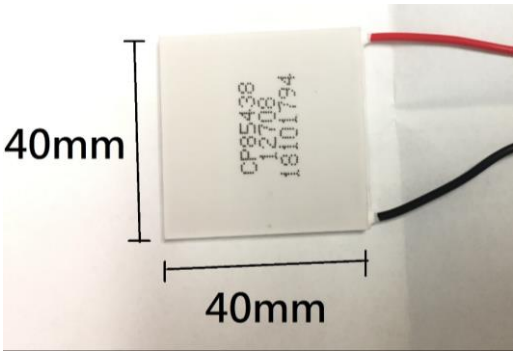

Figure 3 Peltier device CP85438

2.0 Experimental

2.1 Thermoelectric Dehumidifier

The idea of dehumidifying process is trying to condense water while moisture air passing through. As we introduced before TEC has low cost, easily applied and small dimension benefits. Take the model CUI CP85438 for example. The dimension is 40 mm in length and 40 mm in width as well as only 3.7 mm in height. The dehumidifier would be applied on TEC.

2.1.1 Thermoelectric Dehumidifier Design

The thermoelectric dehumidifier contains TEC, heatsink applied in both hot side and cold side, thermal interface materials, desiccant beads, axial fan and acrylic chamber as shown in Figure 4. For increasing cooler surface area omnidirectional heatsink has been introduced in TEC cold side. Cold side cooling structure is placed inside clear acrylic chamber with one inlet and one outlet for collecting condensed water while dehumidifying process. Chamber inlet and outlet are connected to 5/8 inches plastic tubing to humidifier and humidity sensor. The silica gel desiccant at the bottom of chamber is used for moisture absorption. From desiccant comparison graph in Figure 5 silica gel has the best performance at high humidity condition. Also, silica gel has reactivated easily and low cost benefits. During the air purge time the beads are able to soak residual water from the test.

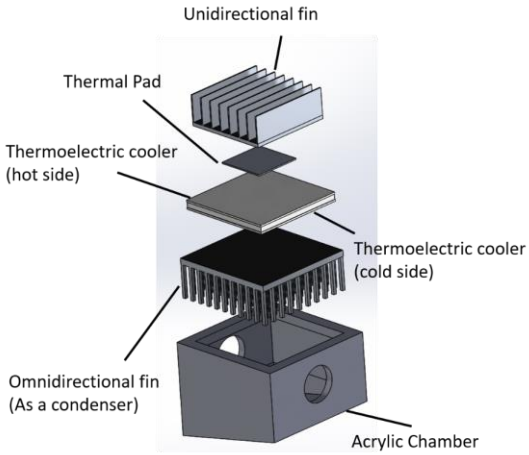

Figure 4 Explosion view for thermoelectric dehumidifier

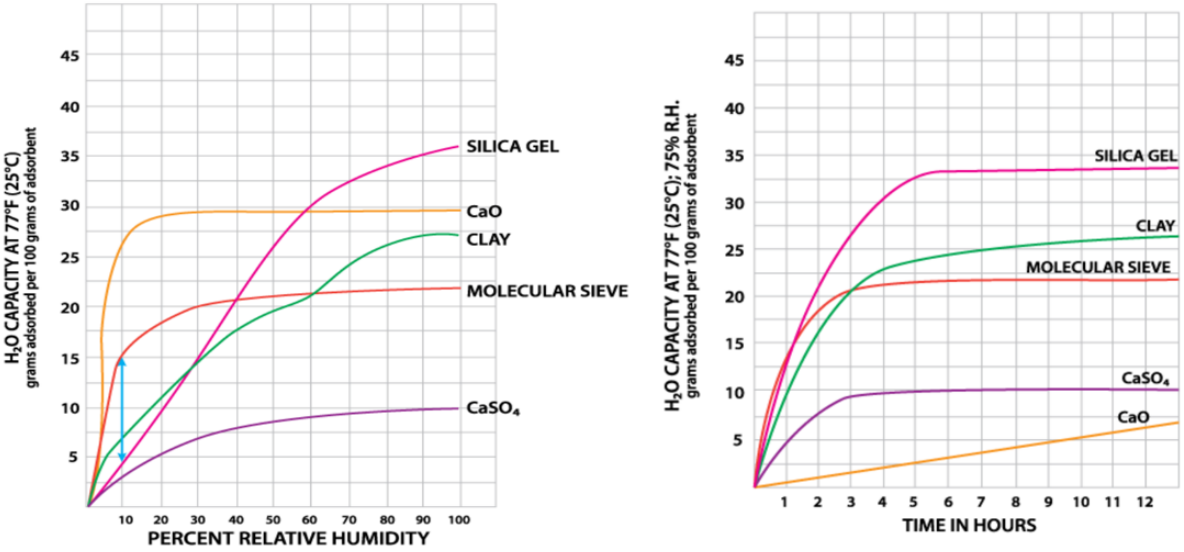

Figure 5 Desiccant comparison

On the other side of the Peltier module when the DC voltage applied on heat energy released on ceramic material substrates which need to be cooled down by external convection. The air cooling axial fan can create maximum 10.8 CFM flow rate which is used for removing released heat from hot side. Same as cold side heatsink increases the contact surface area but this time the thermal interface materials thermal pads are employed for smoothing two dissimilar surfaces thermal resistance. The above parts combinations are our dehumidifier set up. We have two-staged dehumidifiers in serial connection for increasing dehumidified performance. All tubing connections are sealed by hot glues. In terms of simulating human breathing the relative humidity exhale from lung is around 100 percent. The idea for creating high humidity air is evaporating water to form in fine water droplet or foggy like form. Thus, aquarium used disc bubblers and air pump set help increase dissolved oxygen out of water as shown in Figure 6.

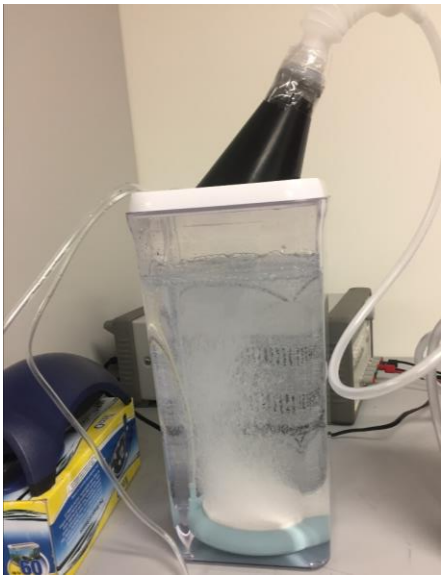

Figure 6 Bubbler humidifier

Be sure that when adding new sections or captions, to return to the table of contents or list of figures/tables and right click on one of the listed items. Then be sure to select Update Field – Update Entire Table, so that any new or edited content is reflected there.

2.1.2 Bubbler Humidifier

For human breath simulation we need to create high humidity air. The idea of making high humidity air is evaporating water to fine or foggy like water drop. Thus, we are using aquarium bubbler with air disk stone and air pump. Bubble is for increasing dissolved oxygen out of water and air pump is for creating desired air flow. The air flow rate also controlled by PVC ball valve.

2.1.3 Experimental Setup

Once the humidified and dehumidified part both settle down, we can start assembling everything. Figure 7 shows the experiment schematic diagram. The collected humid air from bubbler humidifier is connected to ball valve for controlling air flow rate which values measured from flow meter. The dehumidifier outlet is connected to humidity sensor. The assembled thermoelectric dehumidifier is shown in Figure 8.

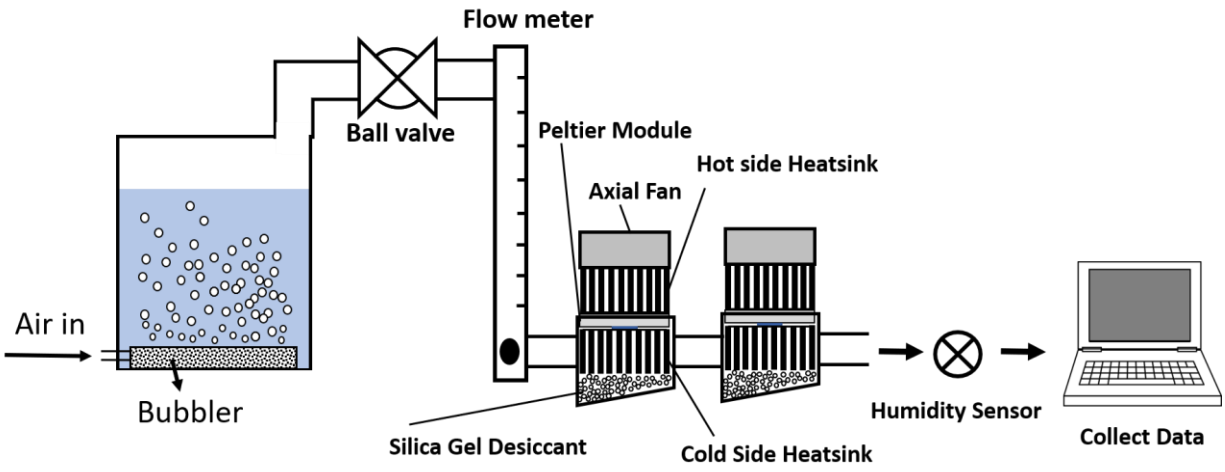

Figure 7 Thermoelectric dehumidifier schematic diagram

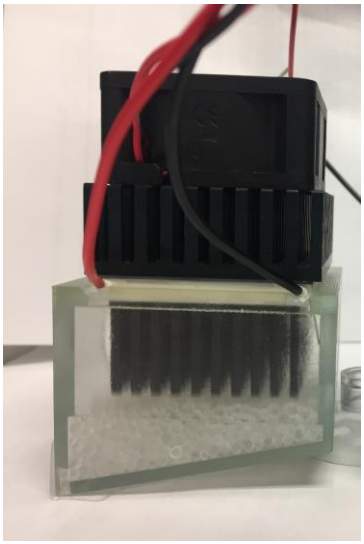

Figure 8 Assembled thermoelectric dehumidifier

2.1.4 Improved Design

The improved dehumidifier is designed for improving air leaking problem. Air leaking in the testing process would lower the acetone sensor sensitivity especially in high relative humidity conditions. According to previous design results, the dead volume from the tubing and connection between 5/8 inches outside diameter VINYL tubing and dehumidifier are the main reason causing system gas leaking. For fixing this problem this time stainless-steel material and narrower diameter tubing have been applied in our system. In order to get robust and stable bonding instead of using hot glue the improved design sealed the boundary with thread connecting. Thus, thread fitting reflect on the new chamber design as shown in Figure 9. The new chamber has extruded boss on both ends for fitting in our 1/4 inches NPT thread. Also, the NPT adaptors are wrapped with Teflon tape for tightening the thread.

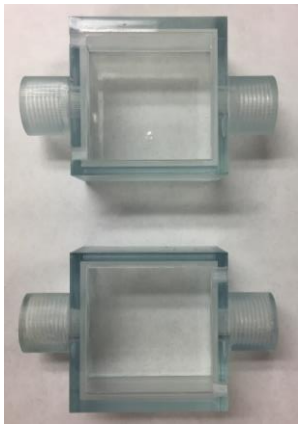

Figure 9 New thread acrylic chamber

Figure 10 Stainless steel tubing

For humidifier part, we cooperated with Bio-Engineering lab they have better equipment for precising the humidity and flow rate. The humidifier setting is shown in Figure 11. The test tube on the Figure 10 is for water and Nitrogen gas mixture. The mixture flow passes through tubing to Cori-Flow (Mass Flow Meter) as in Figure 12(a) where we can setup flow rate from computer. The bottom extruded fitting is fluidic inlet and outlet. Top connector is for power supply connection. Next, the flow goes through Controlled Evaporator and Mixer (CEM) as in Figure 12(b) which also called mixing valve and transforms the liquid and gas into vapor. Once the air and liquid go into CEM the mixing valve atomizes the liquid and heated by CEM. The needle like shape is vapor outlet and the vapor goes into our dehumidifier system.

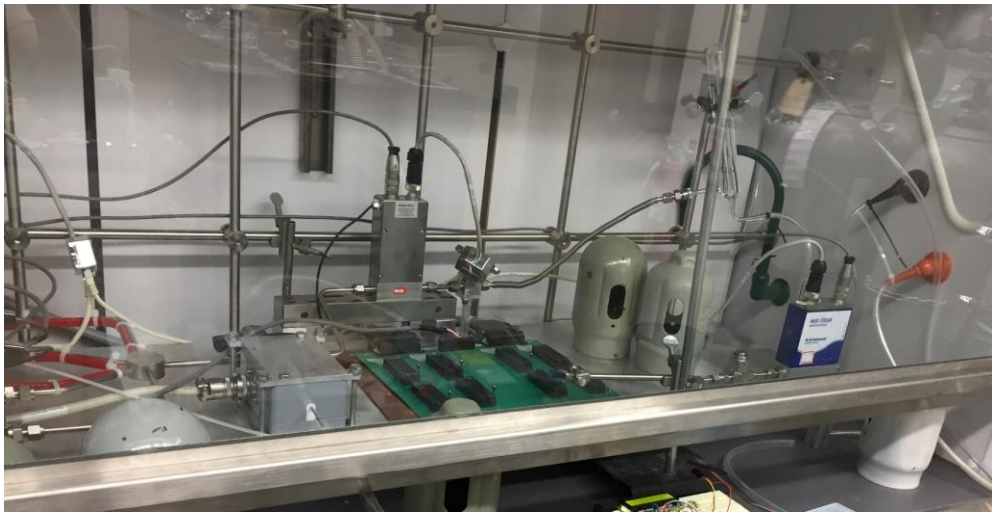

Figure 11 Humidifier setup

Figure 12 (a) Mass flow meter (b) CEM

3.0 Microchannel Dehumidifier

Microchannel dehumidifier is targeting on minimized size for the system which is the second designed dehumidifier in this project. Microchannel dehumidifier help us minimize channel size under micron scale. Microchannel structure is shown in Figure 13. Channel width in between is 500 μm (0.5mm) and the depth is 200 μm. Both inlet and outlet are connected to 1/8 inches PTFB material tubing.

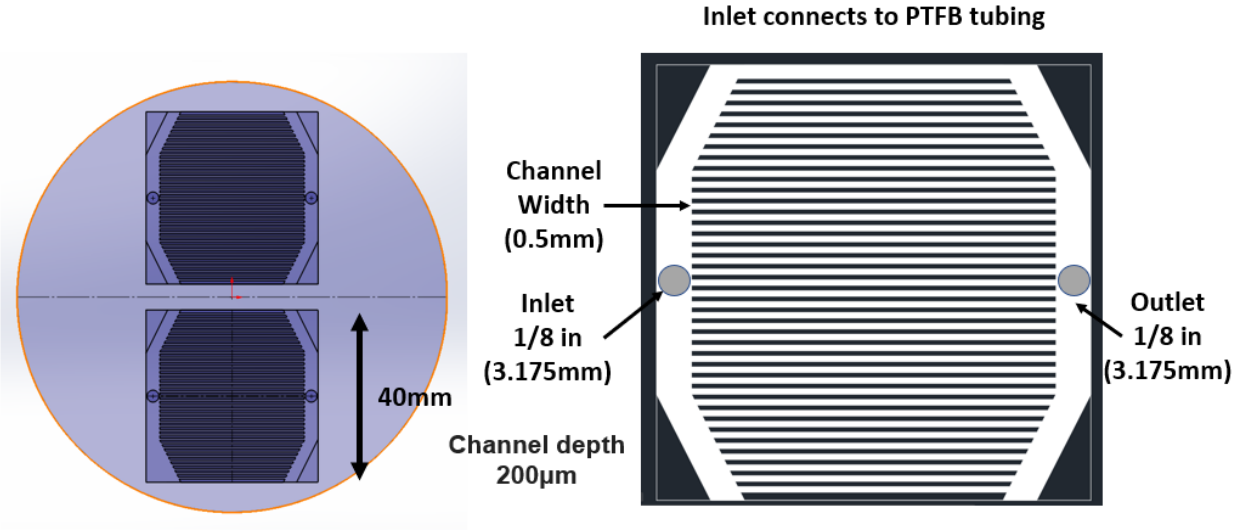

Figure 13 (a) Microchannel on Silicon Wafer (b) Microchannel zoom in

3.1 SU-8 Negative Photoresist

SU-8 negative photoresist is commonly used for making microchannel mold on silicon wafer substrate. The following steps are the processing guidelines. The first step is to clean the substrate surface with H_2SO_4 and H_2O_2 wet etching prior to photoresist process. Second step is coating as we are having film thickness over 200 μm only SU-8 2075 resist can achieve the desired thickness. Different SU-8 series also has different viscosity and density. The higher resist viscosity we pick the thicker PDMS channel can be fabricated. Other than resist series the film thickness also determined by spin speed as shown in Figure 14. For example in this project we are targeting 200 μm thickness according to spin speed versus thickness curve the suitable resist is SU-8 2075 under 1250 rpm spin speed. Usually a lower spinning speed followed by targeting speed. Third step is soft bake for evaporating the solvent and make the photoresist process more solid. Selected film thickness has its corresponding baking time at 65 degree Celsius and 95 degree. Then expose to UV (350-400 nm) radiation for 60 seconds. As we all know UV light can activate photoactive component from SU-8 resist. Once the exposure process done the latent image will reflect on the wafer even without developing. The next step is called Post Exposure Bake (PEB) which is the process right after UV exposure. Like previous soft bake process baking at 65 degree for first few minutes for stress reduction and raise the temperature to 95 degree. After baking the second last step is development. The developer we are using is MicroChem's SU-8 which is recommended for high aspect ratio or thick film structure. The thicker the film the longer the development time needed. After rinsing and drying third and the last photoresist bake is called hard bake. The step prevents cracking by strengthen the SU-8 photoresist at the range of 150 degree to 250 degree lasting for at least 15 mins.

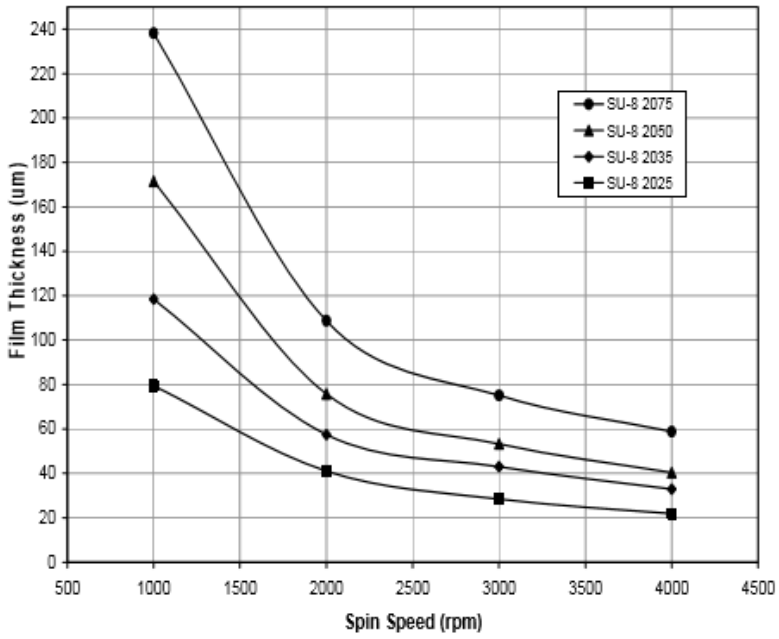

Figure 14 SU-8 spin speed vs flim thickness

3.2 PDMS Fabrication

Polydimethylsiloxane (PDMS) is the material that contains inert, non-toxic and optical clear properties. The fabrication methods for microchannel PDMS is following. First is wrapped silicon wafer mold with aluminum foil before pouring mixture PDMS liquid. Once the mixture PDMS liquid poured onto mold lots of air bubbles generates in the liquid. To remove those bubbles the vacuum desiccator and latches are applied to our process. The next step is heating up mold and PDMS to 150°C for 15 minutes. After heating treatment the fabrication process is basically done. Then peel the microchannel area off the mold and followed by drilling the inlet and outlet with PDMS puncher for tubing connection in the future. Final step is called plasma treatment which

allows PDMS and silicon wafer bonding together for closing the microchannel. The PDMS microchannel is shown in Figure 15(a). The rest of PDMS material and the wafer is shown in Figure 15(b).

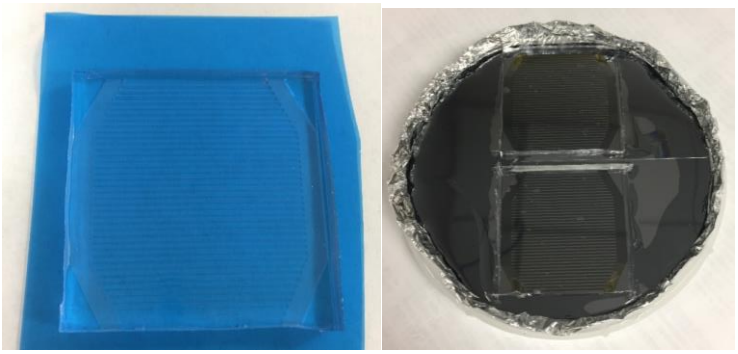

Figure 15 (a) PDMS microchannel (b) PDMS material cut out from silicon wafer

3.3 Applied to System

Two holes on the side are connected to plastic connectors which are the adaptor for 1/8 inches diameter Polytetrafluoroethylene (PTFE) tubing. Inlet hole on PDMS is connected to humidifier where moisture air comes from and the other end to the first-staged dehumidifier as shown in Figure 16. Second hole on PDMS is connected to microchannel outlet and the other end to second-staged dehumidifier. So does second-staged dehumidifier hole but the tubing outlet is connected to humidity sensor or mass spectra for testing air humidity and identifying the contents of the gas stream after passing through two dehumidifiers. The silicon wafer beneath microchannel

will close channel to avoid PDMS material popping off the bonding when dehumidified process working. Plasma is used for bonding between silicon wafer and PDMS microchannel. Silicon wafer in between Peltier device and PDMS not only close channel but also a good interface material in terms of heat conduction. Epoxy is introduced on the bonding of silicon and TEC. With over 3200 psi tensile strength can robust bonding and make sure seal well on the sandwich structure. On the hot side of thermoelectric module we use same heatsink design as previous dehumidifier. The heatsink and external convection fan can remove redundant heat releasing from the plate. According to manual the maximum temperature for hot side plate should not over 80 degree Celsius under any conditions or it will influence the module performance.

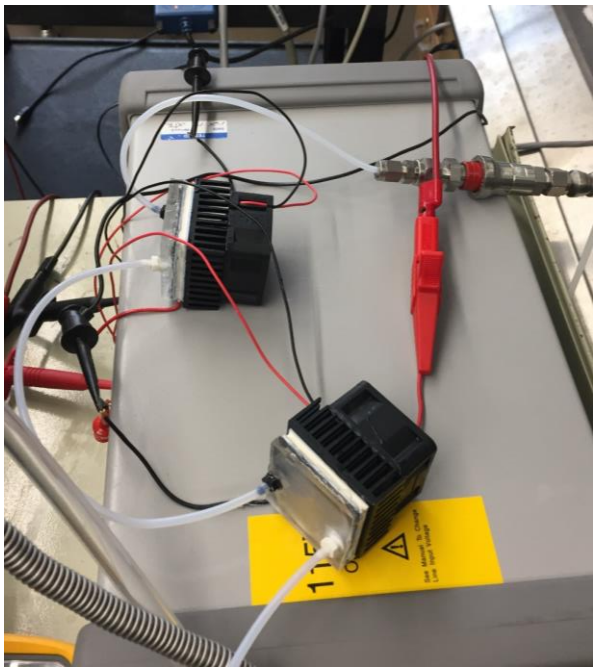

Figure 16 PDMS microchannel system

4.0 Results and Discussion

4.1 Thermoelectric Dehumidifier in Chamber

4.1.1 Arduino Humidity Testing

For the thermoelectric dehumidifier design we are testing humidity level first by Arduino humidity sensor. Human exhale simulation part can reach around 90% Relative Humidity level (%RH). If we raise air pump power to increase flow rate to 19 cubic feet per hour the humidity level can still reach around 85% RH. Once the dehumidifier turned on the humidity level start dropping gradually till approximately 13% RH. Silica gel inside the chamber help remove the residual humidity for repeating test. As the humidity level shown in Figure 17, at 0 to 60 minutes the dehumidifier is turning off. Since we are targeting three humidity levels 20%, 50% and 90% RH at 10 to 20 minutes is testing 20% and 20 to 30 minutes is testing 50% and 30 to 40 minutes is testing 90% humidity. This step helps us make sure our humidity sensor and humidifier working well. After testing sensor and humidifier we start purging air to let the whole system back to dry air condition.

Now we turn on dehumidifier at 60 minutes this time and all the other conditions are same as 0 to 60 mins. By doing so we can compare the humidity changes regarding dehumidifier is on or off. At 75 minutes the humidity level start dropping but still fluctuated till 80 minutes. Then the

difference comes out: The humidity level severely dropped down to around 13% and hold for 10 minutes and then gradually increases. We are guessing the residual moisture inside the chamber influences the dehumidifier performance. But we still can see the huge humidity difference.

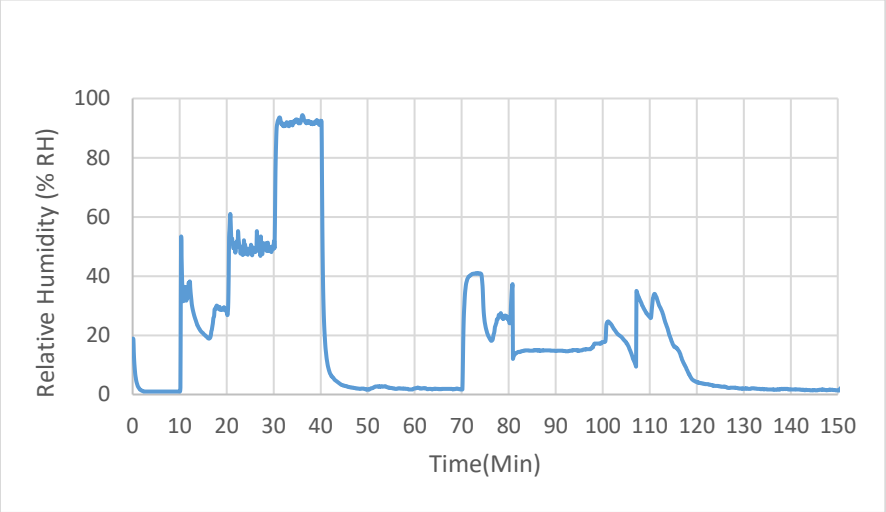

Figure 17 Relative humidity level after thermoelectric dehumidifier applied

4.1.2 Acetone Sensor Testing

After brief humidity level test results from Arduino now the experiment moves on to acetone sensor test. As shown in Figure 18 y axis is normalized current level x axis is our time scale. The current of the sensor drops when there is an increase in the concentration of acetone or the humidity level increases. While in high humidity condition, the humidity reason would dominate on current dropping. Generally, the larger the magnitude of drop in current means greater the concentration of the acetone. On top of the figure the label show that we tested four different

humidity level 0 %, which is dry air condition, 20 %, 50 % and 90 % as well as three different acetone concentration level 1ppm, 10ppm and 100ppm. Each straight solid line interval is 15 minutes with acetone introduced in first 5 minutes followed by 10 minutes purging air in certain humidity level and acetone concentration level. For the dry air condition (0% RH) result shows that the conductivity of sensor decreases and the magnitude of the drop is proportional to the concentration of the acetone. When the sensor is purged with air, the conductivity of the sensor is removed from the sensor surface therefore the current level been recovered. However, when the humidity level is increased to 20% RH it is only able to pick up the signal for 100 ppm concentration level but not at 1 and 10 ppm as shown in Figure 19. The spike disappears when acetone is introduced to the sensor and no current recovery during purging time. The curve is flattened and no current level changes between purging and acetone been introduced. The sensitivity gets worse at higher %RH and the humidity level was held constant even during purge period.

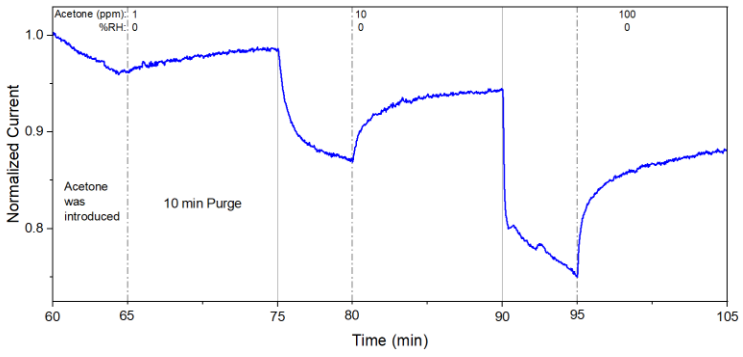

Figure 18 Acetone sensor test at 0% RH condition (Dry air)

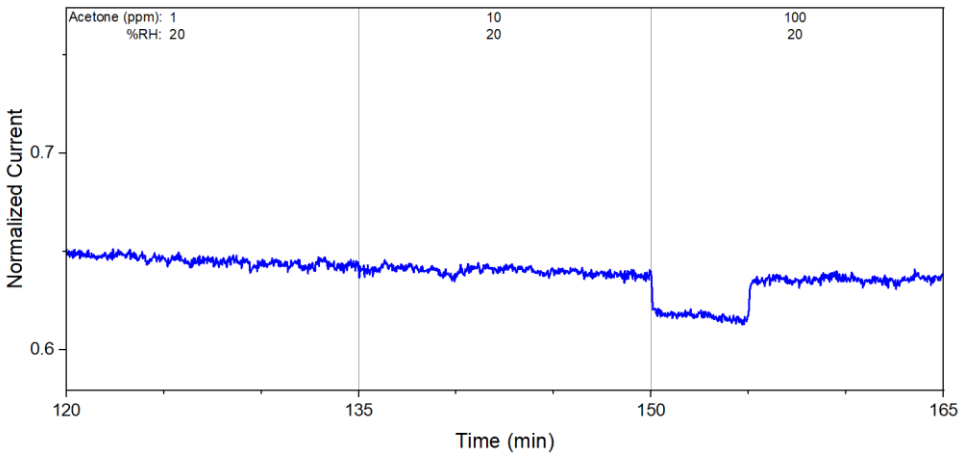

Figure 19 Without dehumidifier system applied on the sensor at 20 % RH

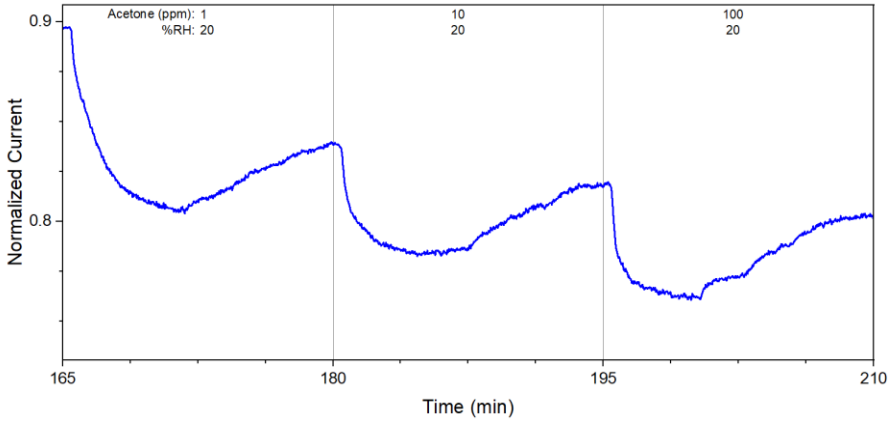

Figure 20 With dehumidifier system applied on the sensor at 20 % RH

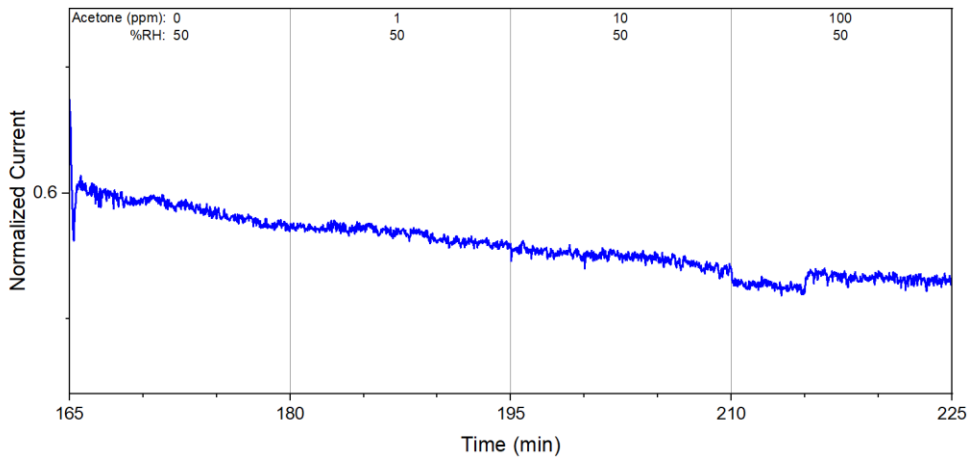

Figure 21 Without dehumidifier system applied on the sensor at 50% RH

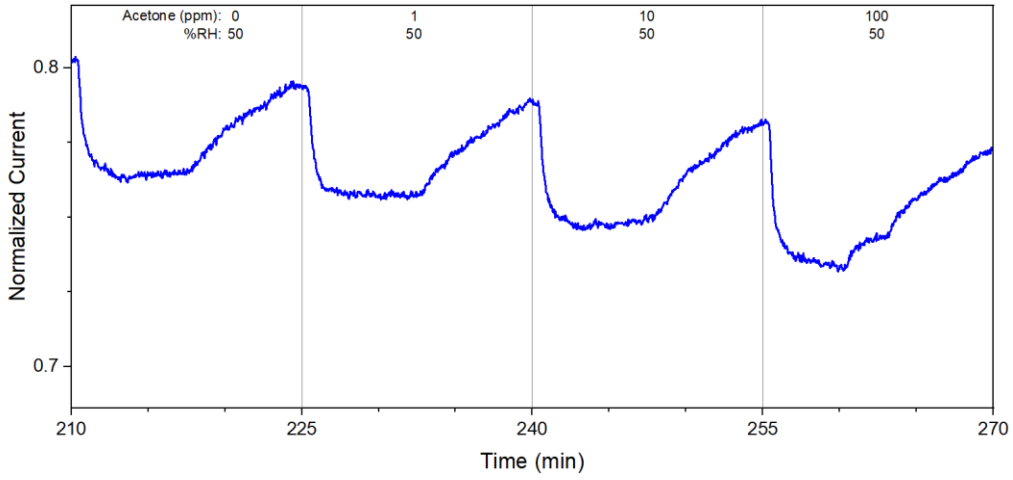

Figure 22 With dehumidifier system applied on the sensor at 50% RH

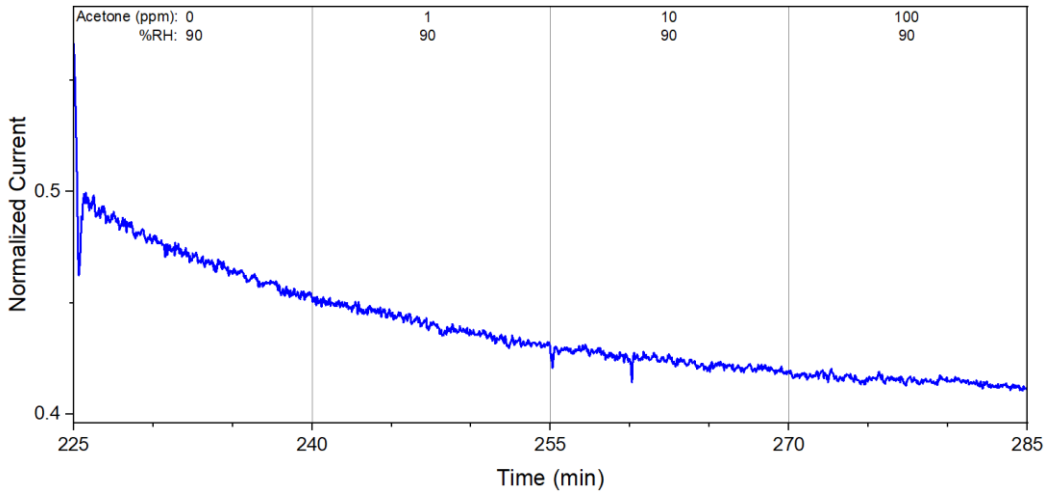

Figure 23 Without dehumidifier applied on the sensor at 90% RH

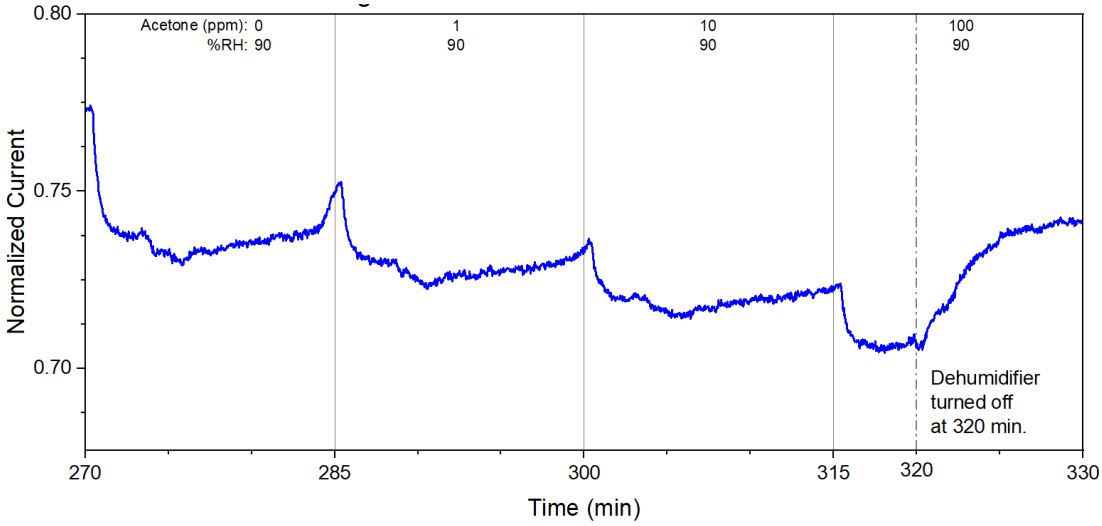

Figure 24 With dehumidifier system applied on the sensor at 90% RH

When comparing to the results that applied dehumidifier few differences stand out. As shown in Figure 20 at 20 % RH dehumidified device can test all three concentration level to 1 ppm concentration. The higher % RH still has reaction and the wave shape looks similar under different

concentration level. However, the response to acetone is diminished even in dry condition and the humidity seems to have less of an effect on the sensor. If we compare 1st derivative plot with and without dehumidifier the results show that a better sensor response to concentration correlation when you focus on the rate of change in current as shown in Figure 25. The sensor sensitivity decreases due to the increase of system dead volume from the tubing, loss of acetone in the connection to dehumidifier and silica gel absorption. Also, the residual humidity can't be removed after few tests even purging with air. This phenomenon can be seen from the mass spectra data collection. The current trace for water remains at a higher level than without dehumidifier indicating that residual humidity left in the dehumidifier. The mass spectra results also showed acetone loss as gas stream passes through the dehumidifier since acetone trace does not increase as much as without applying dehumidifier. Therefore, we have improved dehumidifier design by changing to narrower tubing and use robust stainless steel material and also improve the seal between tubing and dehumidifier.

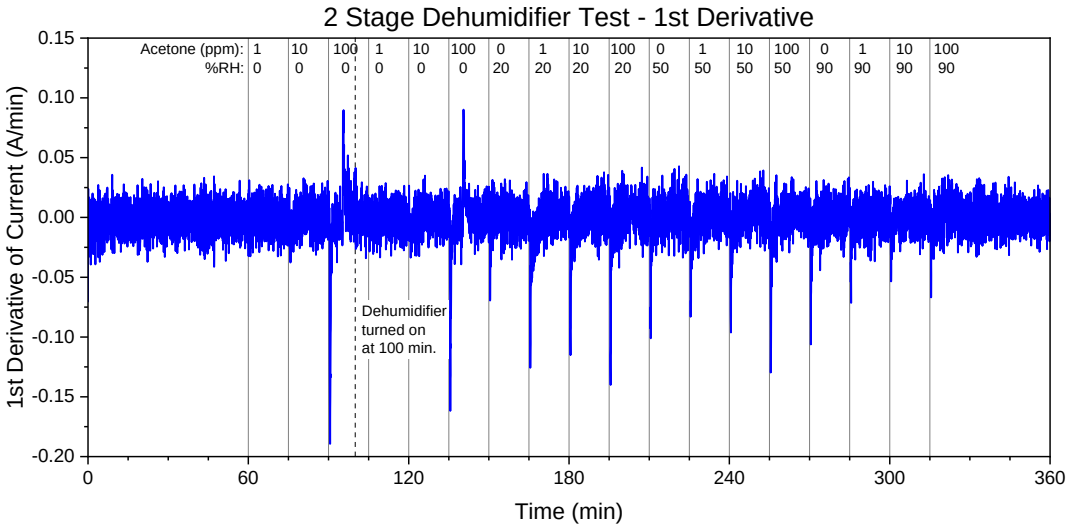

Figure 25 First derivative of acetone current applied on dehumidifier

4.1.3 Mass Spectrometer Test

Figure 26 shows mass spectra data which is collected to identify the contents of the gas stream. The mass spectrometer measures mass to change ratio (m/z) of ionized compounds. In this case Nitrogen (m/z 28), Oxygen (m/z 32), water (m/z 18), and acetone fragment (m/z 43) were monitored over time. As the results showed, when acetone is introduced at the 30, 45, 60, and 90 minute mark, the current increases proportional to the amount of acetone. The current for the other gases also go a bit higher likely due to flow rate changes. The current traces for the water also increases at the 60, 75, 90 minute mark when the humidity in the system goes from 0 to 90%RH.

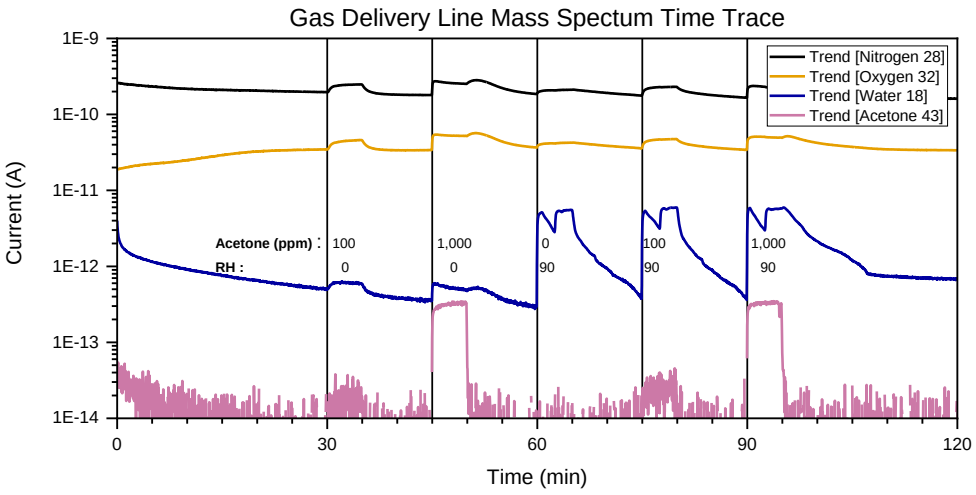

Figure 26 Mass Spectrometer test

4.1.4 Improved Dehumidifier Test

The improved dehumidifier focuses on better sealing and decreases dead volume in tubing. The power supply setting is also changed according to thermoelectric cooler performance plot shown in Figure 27. By increasing current and voltage level would higher heat pumped rate and make more temperature difference. Theoretically, with power supply maximum inputting current at 5A as well as 8 voltage the TEC can make 40 degree difference in cold and hot side. During our temperature test the module hot side reached 45 degree with air cooling fan applied which means cold side temperature is around water freezing point. Just like previous Figure 17 shows that the humidity level changes after dehumidifier applied. The curve gradually increases to three different targeting level (20% RH, 50% RH and 90% RH) until reach 90% RH level.

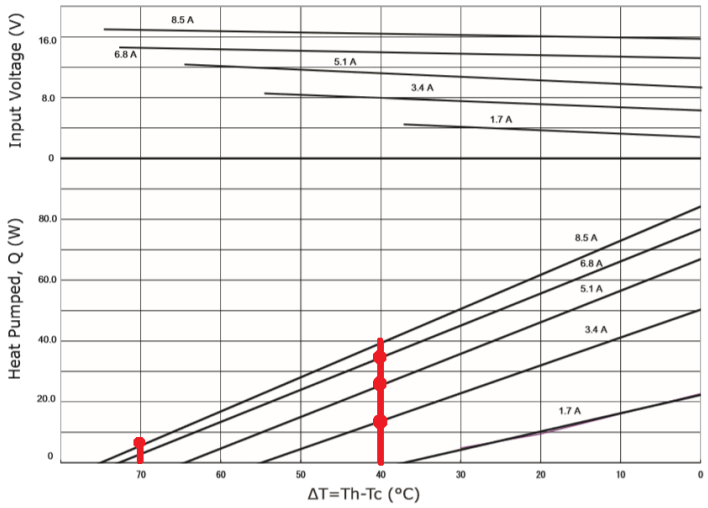

Figure 27 TEC performance with corresponding voltage and current

4.2 PDMS Microchannel Dehumidifier

First, as shown in Figure 28 the dehumidified humidity level change plot after humid air passing through microchannel. Like the section 4.1.1 results TEC chamber test humidifying part starting from dry purge air then raising to 30 % RH, 50 % RH and then turn on dehumidifier. At time 20 to 30 minutes is testing 30% RH and at time 30 to 40 minutes is testing 50% RH. The sudden drop occurs is where air start purging. Then we turn on dehumidifier and all the other factors are same as 0 to 50 minutes. For acetone sensor testing if we compared to non-dehumidified graph the difference stands out. The spike at 70 minutes is acetone introduced to the system just like the one happened at 15 minutes. Then if at 75 minutes the dehumidifier didn't turn on the results supposed to look similar at 20 minutes. But the curve gradually decreases till the lowest point 9% RH and stay stable around 11% for 20 minutes. Finally, we turn off the dehumidifier at 100 minutes and the humidity level back to normal.

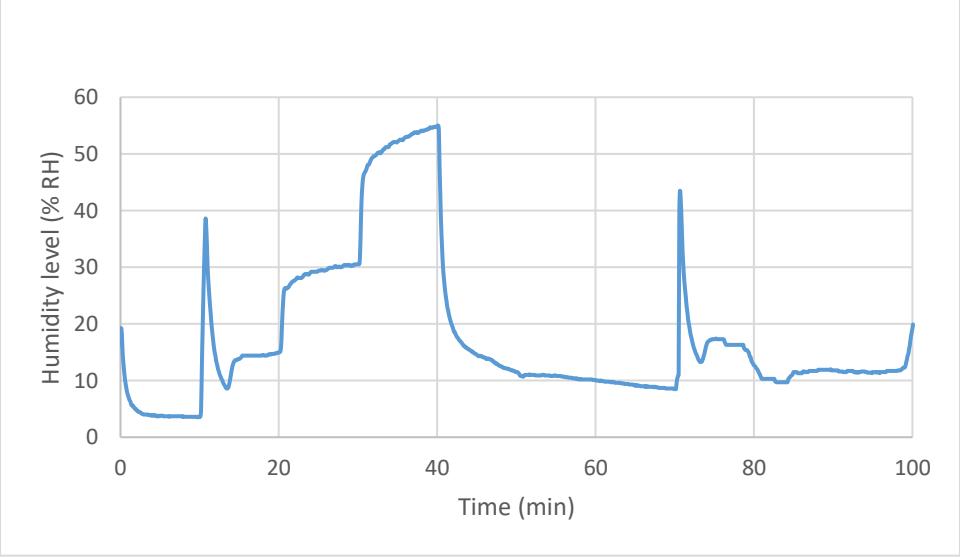

Figure 28 Microchannel dehumidifier humidity change

5.0 Conclusion and Future Work

This thesis presents two different dehumidifier design which improved acetone sensor can work in high humidity level environment which overcomes humidity technical problem while doing human exhale breath test. Furthermore, PDMS microchannel dehumidifier really minimizes the channel size and increases the surface contact area to TEC and better utilizes TEC module.

At this point microchannel dehumidifier can only deal with lower flow rate such as 2 liter per minute. For higher flow rate air passing through our dehumidifier the condensed water would clog channel and it takes more time for air purging or reverse the polarity of the applied voltage to remove water. Although it is acceptable for short period testing it would be a good improvement if we can fix the water clogged problem.

Bibliography

[1] A.Paoli, A.Rubini, J. S.Volek, andK. A.Grimaldi, “Beyond weight loss: A review of the therapeutic uses of very-low-carbohydrate (ketogenic) diets,” *Eur. J. Clin. Nutr.*, vol. 67, no. 8, pp. 789–796, 2013.

[2] J. C.Anderson, “Measuring breath acetone for monitoring fat loss: Review,” *Obesity*, vol. 23, no. 12, pp. 2327–2334, 2015.

[3] T. P. J.Blaikie *et al.*, “Portable device for measuring breath acetone based on sample preconcentration and cavity enhanced spectroscopy,” *Anal. Chem.*, vol. 88, no. 22, pp. 11016–11021, 2016.

[4] Y.Yamada *et al.*, “Ultratrace Measurement of Acetone from Skin Using Zeolite: Toward Development of a Wearable Monitor of Fat Metabolism,” *Anal. Chem.*, vol. 87, no. 15, pp. 7588–7594, 2015.

[5] V.Ruzsányi andM. P.Kalapos, “Breath acetone as a potential marker in clinical practice,” *J. Breath Res.*, vol. 11, no. 2, 2017.

[6] M.Ding, D. C.Sorescu, andA.Star, “Photoinduced charge transfer and acetone sensitivity of single-walled carbon nanotube-titanium dioxide hybrids,” *J. Am. Chem. Soc.*, vol. 135, no. 24, pp. 9015–9022, 2013.

[7] K.Coyne, D.Caretti, W.Scott, A.Johnson, andF.Koh, “Inspiratory flow rates during hard work when breathing through different respirator inhalation and exhalation resistances,” *J. Occup. Environ. Hyg.*, vol. 3, no. 9, pp. 490–500, 2006.

[8] A.You, M. A. Y.Be, andI.In, “A simple calibration methods of relative humidity sensor DHT22 for tropical climates based on Arduino data acquisition system,” vol. 20009, no. January, 2019.

[9] Y.Hongbin, Z.Guangya, C. F.Siong, W.Shouhua, andL.Feiwen, “Novel polydimethylsiloxane (PDMS) based microchannel fabrication method for lab-on-a-chip application,” *Sensors Actuators, B Chem.*, vol. 137, no. 2, pp. 754–761, 2009.

[10] H.Al-madhhachi andG.Min, “Effective use of thermal energy at both hot and cold side of thermoelectric module for developing efficient thermoelectric water distillation system,” *Energy Convers. Manag.*, vol. 133, pp. 14–19, 2017.

[11] J.Kim, K.Park, D.Lee, Y. S.Chang, andH.Kim, “Optimal cold sink temperature for thermoelectric dehumidifiers †,” vol. 32, no. 2, pp. 885–895, 2018.